Capillary Pumping between Droplets on Superhydrophobic Surfaces

Journal:	*AIChE Journal*
Manuscript ID	AIChE-21-24502
Wiley - Manuscript type:	Research Article
Date Submitted by the Author:	01-Nov-2021
Complete List of Authors:	moradi, shiva Charsooghi, Mohammad Businaro, Luca; Institute of Photonics and Nanotechnologies National Research Council, Habibi, Mehdi; Wageningen Universiteit en Researchcentrum, Moradi, Ali-Reza; Institute for Advanced Studies in Basic Sciences, Physics
Keywords:	Capillary pumping, Droplets, Superhydrophobic surface

ORIGINAL ARTICLE

Journal Section

Capillary Pumping between Droplets on Superhydrophobic Surfaces

Shiva Moradi Mehr[1] | **Mohammad A. Charsooghi**[1] | **Luca Businaro**[2] | **Mehdi Habibi**[3] | **Ali-Reza Moradi**[1,4]

[1]Department of Physics, Institute for Advanced Studies in Basic Sciences (IASBS), Zanjan 45137-66731, Iran

[2]Italian National Research Council - Institute for Photonics and Nanotechnologies (CNR - IFN), via Cineto Romano 42, 00156 Rome, Italy

[3]Physics and Physical Chemistry of Foods, Wageningen University, 6700 AA Wageningen, The Netherlands

[4]School of Nano Science, Institute for Research in Fundamental Sciences (IPM), Tehran 19395-5746, Iran,

Correspondence
Ali-Reza Moradi, Ph.D., Department of Physics, Institute for Advanced Studies in Basic Sciences (IASBS), Zanjan 45137-66731, Iran
Email: moradika@iasbs.ac.ir

Funding information

The famous two-balloon experiment involves two identical balloons filled up with air and connected via a hollow tube, and upon onsetting the experiment one of the balloons shrinks and the other expands. Here, we present the liquid version of that experiment. We use superhydrophobic (SHP) substrates to form spherical droplets and connect them with a capillary channel. Different droplet sizes, substrates of different hydrophobicities, and various channel pathways are investigated, and morphometric parameters of the droplets are measured through image processing. In the case of SHP substrates the pumping is from the smaller droplet to the larger one, similar to the two-balloon experiment. However, if one or both of the droplets are positioned on a normal substrate the curvature radius will indicate the direction of pumping. We interpret the results by considering the Laplace pressures and the surface tension applied by the channel at the connecting points.

KEYWORDS
Capillary pumping, Droplets, Superhydrophobic surface

1 | INTRODUCTION

Microfluidic systems have emerged as a distinct field in lab-on-a-chip technology where handling small volumes is critical, and the capability to drive and manipulate fluids has led to industrial and biological applications [1, 2]. For

Abbreviations: SHP, Superhydrophobic; SW, Silicon Wafer.

several chemical and biological analyses and recognition the use of droplets is required, and pumping using droplets for microscale transport in a microchannel has been an alternative microfluidic approach to create fluidic pathways [1, 3]. In this paper, we present experimental investigation of the fluidic micropumping on a superhydrophobic patterned surface (SHP), i.e. non-wettable surfaces with water contact angle higher than 150°. This, indeed, is very similar to the so-called two-balloon experiment. In that experiment, two identical balloons are inflated to different diameters and connected by means of a hollow tube. The flow of air through the tube can be controlled by a valve or clamp. When the valve is opened or the clamp is released, air is allowed to flow between the balloons. For many starting conditions, the smaller balloon gets smaller and the balloon with the larger diameter expands even more. This result is surprising, since most people assume that the two balloons will have equal sizes after exchanging air. The behavior of the balloons was first explained theoretically by David Merritt and Fred Weinhaus in 1978 [4]. The liquid version of the balloons can be resembled by spherical shaped droplets. These droplets can be formed on SHPs.

Lotus leaves and rose petals are the examples of naturally occurring SHP surfaces. By mimicking such systems artificial surfaces, on which microliter sized water droplets have an almost spherical shape, have been developed [5, 6]. The very high contact angle of a water droplet resting on these surfaces is a consequence of surface chemistry and the presence of a micro and nanoscopic rough surface texture [7]. SHP surfaces have found important applications for anti-wetting and self-cleaning materials [8, 9]. More importantly, they are promoting technological advancements in biology and medicine, with a variety of potential applications in diagnostic and therapeutic practice [10, 11, 12, 13]. For example, SHP surfaces have enabled separation of biological mixtures [14], improvement of ultrasensitive molecular spectroscopy [15], smart chemical reactors [16], and controlling drug release [17, 18], to name a few.

Concerning the aforementioned important applications, here, on SHP surfaces, we investigate the phenomenon of micropumping, which is one of the main developing areas in microfluidics and lab-on-a-chip technology. The development of principles for the pumping and fabrication of pumping instrumentations has attracted interests due to their use in procedures such as blood chemistry analysis, flow cytometry, polymerase chain reactions and DNA screening [19, 20]. Several methods have been suggested to pump fluids into microchannels [21, 20, 22]. Amongst, the simplest methodology is taking the advantage of intrinsic features of microfluidic channels such as surface tension, molecular diffusion and osmotic pressure. The pumping onset and its rate will depend on the Laplace pressure difference between the two sides of the interconnecting microchannel, which, in turn, might be a function of the aforementioned features as well as the length and pathway of the microchannels [23]. In this study, we propose a systematic investigation of these parameters on the micropumping between droplets. First, in order to resemble the liquid version of the two balloon experiment, we focus on the micropumping between two droplets of different sizes at rest on SHP surfaces. Then, we extend the study to consider the cases of normal substrates for one or both of the droplets. We use silicone wafer (SW) as a normal substrate.

2 | MATERIALS AND METHODS

The SHP surfaces we use in the experiments are artificial biomimetic rough surfaces. These substrate are fabricated on a 100 silicon wafer (SW) by electron beam lithography (Vistec EPBG-5HR acceleration voltage: 100 keV) and inductive coupled plasma (ICP) Si etching. First, a layer of Shipley UVIII electronic resist with the thickness of 1.2 μm is spun on the silicon surface, and then it is exposed to a dose of 25 μC/cm^2 and finally it is developed. The device pattern is an array of pillars of 5 μm side and 14 μm pitch, which is defined by deposition and lift-off a thin Cr film (30 nm thickness). The device pattern is transferred on the substrate by a two-steps ICP Si etching. In the first step (protection), the parameters are kept as pressure=100 mTorr, Ar=30 sccm, C4F8=187 sccm, ICP= 600 Watt, t=2 s, and in the second step

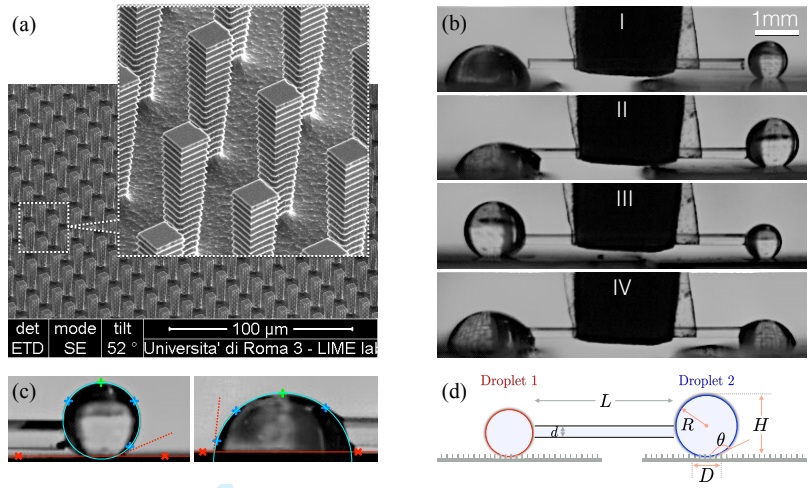

FIGURE 1 (a) A SEM tilted image ($52°$) and its magnified view of the fabricated SHP substrate; (b) The configurations of micro-pumping experiments. Arrangements I and II: water droplets on the left and right sides are placed on SW and SHP surfaces, respectively. In I the SW droplet and in II the SHP droplet is the bigger one. Arrangements III and IV: the droplets both are placed on SHP and SW surfaces, respectively; (c) Finding the best fitted circle to the 2D images of the side view of the droplets; (d) Definition of the investigated morphometric parameters: D: contact line, θ: contact angle, H: height, R: curvature radius, d: capillary inner diameter, L: length of the capillary tube.

(etching), as pressure=100 mTorr, Ar=100 scccm, SF6=90 sccm, cathode bias=70 V, ICP=500 Watt, t=10 s. As for the saw-shaped pillars array, a 400 nm thick layer PMMA 950K 9% is spun on a SW, exposed with a dose of 700 μC/cm^2 and developed. A 30 nm thick Cr film is then deposited by e-gun assisted evaporator and lifted off. The device pattern is transferred on the substrate by the same ICP etching procedure. After cleaning in Piranha solution (H_2SO_4/H_2O_2=3:1), both microstructured SWs are salinized to impart the SHP behavior with 10% trimethylchlorosilane in toluene. The resulting surface show a contact angle for DI water $\theta > 150°$ and a roll off angle $< 4°$. The SHP areas are fabricated in four different zones of 6 mm$\times$6 mm distanced by 4 mm from each other. The rest of the silicone surface remain unpatterned and is used for the experiments in which one or both substrates is a normal substrate. In order to perform the SHP-SHP micro-pumping experiments, the device is cut into two identical parts. In Fig. 1a a SEM tilted image ($52°$) along with its magnified view of the fabricated sample is shown.

Figure 1 b shows the various configurations of micro-pumping experiments carried out in this research. Two droplets of required sizes are positioned on separate SHP or SW surfaces using a micropipette. In both arrangements of I and II water droplets on the left and right sides are placed on SW and SHP surfaces, respectively. However, in arrangement I the SW droplet and in arrangement II the SHP droplet is the bigger one. In arrangements III and IV both droplets are placed on SHP and SW surfaces, respectively.

The droplets get connected via a capillary micro-tube (VitroTubes$^{\text{TM}}$) of 5 mm length and three different inner diameters of 150 μm, 400 μm, and 650 μm. To avoid capillary force driven flow of the droplets, initially the capillary is filled-up. The surfaces are placed on micro-positioners, and by their adjustments the two droplets come close to the ends of the capillary to create flow. Upon the connection of the capillary to the droplets initial oscillations of the droplets are observed. These oscillations are more pronounced for the larger droplets since the inertial and gravitational forces enhance by increasing the droplet size [24]. In order to avoid their effects on the results, the initial frames are excluded for the analysis.

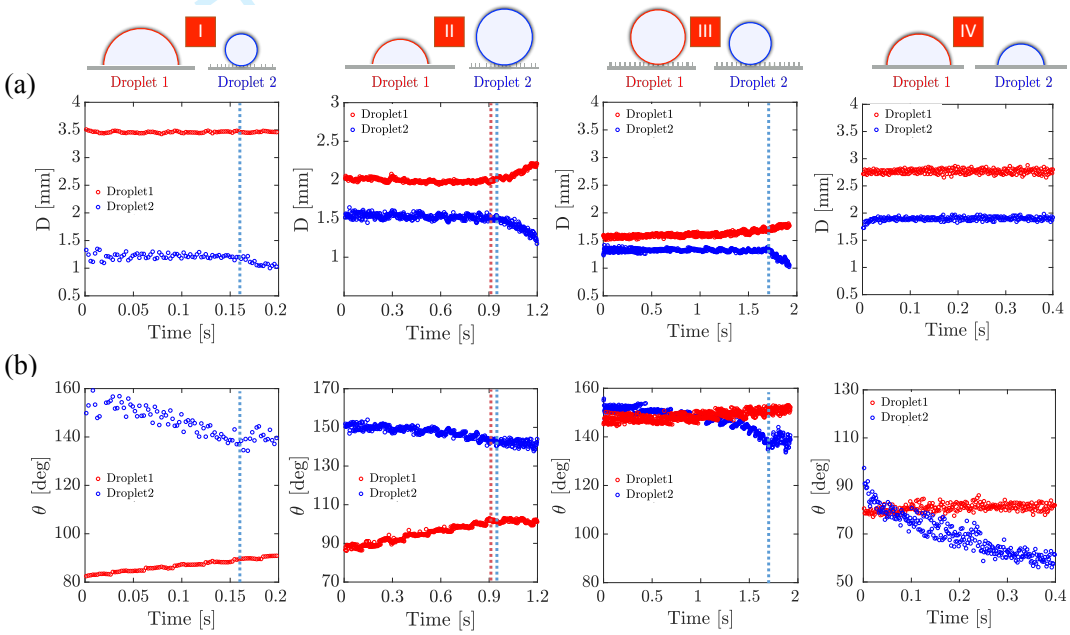

FIGURE 2 Image processing results; Time evolution of (a) contact line and (b) contact angle of the two droplets. (I): larger droplet on SW and smaller one on SHP; (II): larger droplet on SHP and smaller one on SW; (III): both of the droplets on SHP; (IV): both of the droplets on SW. The vertical dashed lines indicate the changes from one mode (CCL or CCA) to the other mode (CCA or CCL).

3 | EXPERIMENTAL RESULTS AND DISCUSSION

So far several active pumping methods for moving the fluid inside microchannels have been developed [22, 25], however most of them require complex arrangements. Instead, in the passive micro-pumping arrangement, which is considered in this research, the intrinsic property of droplets and their surface tensions drive the pumping and there is no need for external forces [26]. We repeat the pumping experiments several times for the four arrangements of I, II, III, IV, shown in Fig. 1b. The independent control on the size and position of the two droplets, i.e., droplet-droplet relative distance and droplets-capillary relative heights and distances, provides a suitable platform to investigate various parameters involved in the micro-pumping phenomena. The analysis is based on image processing. Evolution of the two droplets during the flow are captured by video imaging using a digital camera (DCC1545M, Thorlabs, 8 bit dynamic range, 5.2 μm pixel pitch) at 400 fps frame rate for a selected region of interest. The recorded movies are converted into image sequences and post-processed to extract the morphometric parameters of the droplets. The measured morphometric parameters of the droplets are diameter of contact area or contact line (D), contact angle (θ), radius of curvature (R), height (H) and volume (V). The image analysis is performed using a MATLAB® code by finding the best fitted circle to the 2D side view images of the droplets (Fig. 1c). In Fig. 1d the investigated morphometric parameters are defined. As it will be shown in the following, considering the measured values of these parameters for several experiments, we observe similar trends in the identical experimental conditions. These conditions include adjusting the initial volume of the droplets placed on the substrates, using capillaries of identical length and inner diameter, and preserving the environmental parameters such as temperature and humidity of the lab.

The time evolution results of the morphometric parameters are summarized in Figs. 2 and 3. The aforementioned four arrangements are schematically shown on top of the figures for easy comparisons. The initial contact angles for the SHP and the SW surfaces are $157^\circ \pm 4^\circ$ and $89^\circ \pm 4^\circ$, respectively. We conduct the experiments for three capillary tubes of different inner diameters. Results show similar behavior, however, the pumping is generally faster for the bigger diameters. Supplementary video 1 compares the pumping velocities on SHP surfaces for three different inner diameters of the connecting capillary tubes.

Upon placing two droplets of unequal sizes (volumes) at the two ends of the microchannel and, more importantly, on the surfaces of identical properties, the surface tension between the droplets and the capillary drives fluid flow from a droplet to the other one. Moreover, the surface tension between the droplet and the surface is also an interfering parameter, and has an impact mainly for the SW case, because of the small contact line for the SHP case. The transport analysis is conducted by placing different volumes of droplets on the SHP and SW surfaces. According to the Laplace law, similar to the two balloon experiment, the flow direction is determined knowing that the two droplets with different curvature radii have different capillary pressures; Small droplet, which as a consequence of the Young-Laplace equation has higher internal pressure, is spontaneously directed to merge into the large droplet which has a lower internal pressure causing fluid flow. We observe two modes for a droplet which is placed on a surface and subjected to pumping: constant contact line (CCL) mode (theta changing - increasing or decreasing), and constant contact angle (CCA) mode (D changing - increasing or decreasing). The vertical dashed lines indicate the changes from one mode to the other mode. Even if the flow direction should be explained by considering the Laplace pressure difference between the two droplets, however, if the surfaces are different, then further factors may also play roles and the behavior on various states and modes are some issues to be discussed. The pressure difference between the droplets, ΔP, in all the cases can be calculated from the Young-Laplace equation, $\Delta P = 2\gamma(\frac{1}{R_R} - \frac{1}{R_L})$, where γ is the surface tension coefficient and R_R and R_L are the radii of curvature of the connecting droplets. Alternatively, the theoretical prediction for a steady state flow in a channel with circular cross-section provides calculation of the pressure difference through measurement of the flow rate between the droplets [27], $\Delta P = Q(\frac{8\eta L}{\pi a^4})$, where Q is the flow rate, L is the length of the channel, η is the

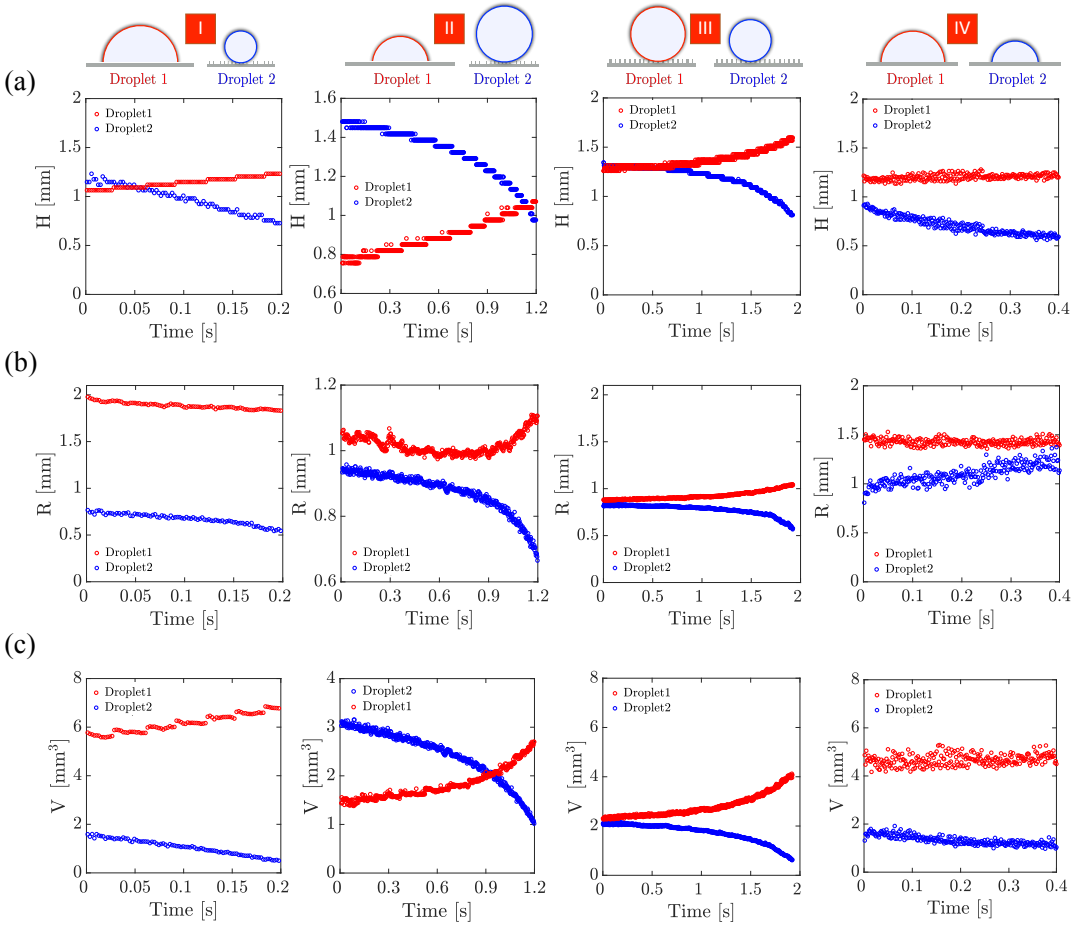

FIGURE 3 Image processing results; Time evolution of (a) height, (b) curvature radius, and (d) volume of the two droplets. (I): larger droplet on SW and smaller one on SHP; (II): larger droplet on SHP and smaller one on SW; (III): both of the droplets on SHP; (IV): both of the droplets on SW.

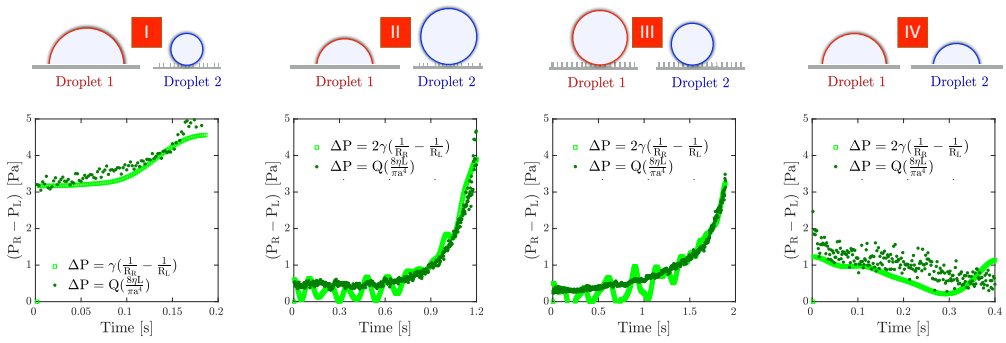

FIGURE 4 Laplace pressure difference of the two droplets. (I): larger droplet on SW and smaller one on SHP; (II): larger droplet on SHP and smaller one on SW; (III): both of the droplets on SHP; (IV): both of the droplets on SW.

viscosity of water, and $a = \frac{d}{2}$ is the radius of the channel.

We observe that if the droplets are placed on different substrates, cases I and II, the flow onsets from the droplet with smaller R to the higher R, regardless of their volume. The curvature radius, hence, is the determining factor rather than the volume and consequently most of the time the flow is from the droplet on SHP to the one on SW. However, in some cases in which the flow direction is from the droplet on SW to the one on SHP, in the midway the flow direction is changed to SHP-to-SW (Supplementary video 2). Back flow phenomenon may be explained by considering the surface tension [28, 29, 26]. Generally, a droplet on a SHP or even on a SW surface experiences both CCL and CCA modes in capillary pumping, provided that the variation of the droplet size in the course of the experiment is sufficiently large. Otherwise, the droplet will be pumped out or get inflated in a mode before experiencing the other mode. The time to change the mode from CCL to CCA or from CCA to CCL varies and depends on the surface properties, the speed of flow, and the relative sizes of the droplets. These parameters, themselves, depend on the capillary inner diameter and length, the hydrophobicity and chemistry of the surfaces, and the environmental conditions. To verify this we consider several arrangements, such as, placing droplets of different sizes, large and small size differences, placing droplets on two different surfaces, and using different capillary diameter and length.

Our results, collectively, show that curvature radius governs the direction of flow, not the volume. In the cases III and IV, when the droplets are placed on identical surfaces, comparing the volumes also leads to the same conclusion for flow direction. When the size of the droplets are rather big the gravitation force tends to bring them into an ellipsoidal shape. Nevertheless, in our experiments the sizes are small enough to keep the spherical shape assumption. On the other limit, when the size of the droplet is very small, the droplets take irregular shapes and fitting a circular function to their lateral side images is erroneous. In order to avoid errors we do not consider such cases in image processing and follow the pumping as long as a reliable circle fitting is possible. In Fig. 2, case I, at the beginning of the experiment D has a much larger value, which is because of being on SW surface and having a rather big initial volume. In contrary θ is much smaller. In case III, the sizes are chosen to be only slightly different which leads to slower capillary pumping. As expected, the variations of volume and height follow a similar trend. The discontinuity (step-like) in the figures is due to the image processing procedure and it originates from the fact that H has a slowly varying trend in all cases. If the changes in H is less than a pixel size in an image, then the change is rounded to zero or one pixel and cause the step-like behavior in H and all the parameters related to H.

Generally in passive pumping the total pressure difference between the two ends of pumping system may include also the hydrostatic pressure difference term and a pressure term due to the inertia terms in the droplet [30]. The

pressure difference, and hence, the pumping rate depends also on the flow properties, droplet shapes, and geometrical characteristics of the channel [30, 27]. However, in our setup, all the affecting parameters are preserved and only the influence of surface hydrophobicity has been the main concern. Fig. 4 shows the calculated pressure differences between the droplets in the course of capillary pumping for all the studied cases. Light green squares and dark green circles show the calculated pressure differences through the $\Delta P = 2\gamma(\frac{1}{R_R} - \frac{1}{R_L})$ and $\Delta P = Q(\frac{8\eta L}{\pi a^4})$ equations, respectively. The flow rate is derived by the differentiation on the measured volume values. In cases I, II and III, the pressure difference follows a similar trend as either both or one of the droplets experience both CCL and CCA pumping modes. However, in case IV, where the both droplets are on SW surfaces, they experience only the CCL mode. Hence, since the change in volume is mainly due to the change in the contact angles (especially for the bigger droplet) their radii of curvature and, therefore, their pressures approach to each other. Our observations especially for the SHP-SHP case are in agreement with the two balloon experiment. Discrepancies seen between two sets of Laplace and flow rate methods are likely due to the initial assumption of long channel length to guarantee the steady state flows in channels and the effect of reflected light and other noises on the fitting and measurements in image processing stage.

4 | CONCLUSION

In conclusion, we investigated experimentally the passive capillary pumping between two droplets of different sizes placed on surfaces of different hydrophobicity. In the case that both surfaces are superhydrophobic the experiments resemble the liquid version of the famous two balloon experiment. Our results collectively show that the pumping rate depends on the microchannel pathway and surface tension in their entrance, shape of the two droplets, which is a function of the hydrophobicity of the surfaces they are placed, and more importantly the relative curvature radii of the droplets. It is demonstrated that if one of the droplets deposits on the hydrophobic surface, it is the curvature that determines the direction of the flow not the volume, and the flow is always from the droplet with smaller radius of curvature to the larger radius of curvature. The experimental results can be explained considering the Laplace pressure equation. Experimental results also demonstrate that the volume changes of the two droplets occurs in two characteristic modes: constant contact angle and constant contact line modes, and smaller pathway diameter of the connecting tubes results in greater flow resistances and causes fluid to flow slower. An important capability of the presented arrangement is that the two connected droplets can be held in completely different environmental conditions. Therefore, it provides a versatile tool, for example, to study thermo-capillary phenomenon which involves a convective flow [31] or other active methods of controlling surface tension driven flows.

ACKNOWLEDGEMENTS

Shiva Moradi Mehr appreciates the partial support provided by the Iran National Science Foundation (INSF).

REFERENCES

[1] Chiu DT, Demello AJ, Di Carlo D, Doyle PS, Hansen C, Maceiczyk RM, Wootton RC. Small but perfectly formed? Successes, challenges, and opportunities for microfluidics in the chemical and biological sciences. Chem. 2017 Feb 9;2(2):201-23.

[2] Cui P, Wang S. Application of microfluidic chip technology in pharmaceutical analysis: A review. Journal of pharmaceutical analysis. 2019 Aug 1;9(4):238-47.

[3] Kaminski TS, Garstecki P. Controlled droplet microfluidic systems for multistep chemical and biological assays. Chemical Society Reviews. 2017;46(20):6210-26.

[4] Merritt DR, Weinhaus F. The pressure curve for a rubber balloon. American Journal of Physics. 1978 Oct;46(10):976-7. latthe2014superhydrophobic

[5] Latthe SS, Terashima C, Nakata K, Fujishima A. Superhydrophobic surfaces developed by mimicking hierarchical surface morphology of lotus leaf. Molecules. 2014 Apr;19(4):4256-83.

[6] Ciasca G, Papi M, Businaro L, Campi G, Ortolani M, Palmieri V, Cedola A, De Ninno A, Gerardino A, Maulucci G, De Spirito M. Recent advances in superhydrophobic surfaces and their relevance to biology and medicine. Bioinspiration, biomimetics. 2016 Feb 4;11(1):011001.

[7] Shirtcliffe NJ, McHale G, Atherton S, Newton MI. An introduction to superhydrophobicity. Advances in colloid and interface science. 2010 Dec 15;161(1-2):124-38.

[8] Jung YC, Bhushan B. Contact angle, adhesion and friction properties of micro-and nanopatterned polymers for superhydrophobicity. Nanotechnology. 2006 Sep 15;17(19):4970.

[9] Kijlstra J, Reihs K, Klamt A. Roughness and topology of ultra-hydrophobic surfaces. Colloids and Surfaces A: Physicochemical and Engineering Aspects. 2002 Jul 9;206(1-3):521-9.

[10] Ueda E, Levkin PA. Emerging applications of superhydrophilicsuperhydrophobic micropatterns. Advanced Materials. 2013 Mar 6;25(9):1234-47.

[11] Lima AC, Mano JF. Micro-/nano-structured superhydrophobic surfaces in the biomedical field: part I: basic concepts and biomimetic approaches. Nanomedicine. 2015 Jan;10(1):103-19.

[12] Lima AC, Mano JF. Micro/nano-structured superhydrophobic surfaces in the biomedical field: part II: applications overview. Nanomedicine. 2015 Jan;10(2):271-97.

[13] Gentile F, Coluccio ML, Limongi T, Perozziello G, Candeloro P, Di Fabrizio E. The five Ws (and one H) of super-hydrophobic surfaces in medicine. Micromachines. 2014 Jun;5(2):239-62. gentile2011nanoporous

[14] Gentile F, Coluccio ML, Accardo A, Asande M, Cojoc G, Mecarini F, Das G, Liberale C, De Angelis F, Candeloro P, Decuzzi P. Nanoporous-micropatterned-superhydrophobic surfaces as harvesting agents for few low molecular weight molecules. Microelectronic Engineering. 2011 Aug 1;88(8):1749-52.

[15] De Ninno A, Ciasca G, Gerardino A, Calandrini E, Papi M, De Spirito M, Nucara A, Ortolani M, Businaro L, Baldassarre L. An integrated superhydrophobic-plasmonic biosensor for mid-infrared protein detection at the femtomole level. Physical Chemistry Chemical Physics. 2015;17(33):21337-42.

[16] Accardo A, Burghammer M, Cola ED, Reynolds M, Fabrizio ED, Riekel C. Calcium carbonate mineralization: X-ray microdiffraction probing of the interface of an evaporating drop on a superhydrophobic surface. Langmuir. 2011 Jul 5;27(13):8216-22.

[17] Yohe ST, Colson YL, Grinstaff MW. Superhydrophobic materials for tunable drug release: using displacement of air to control delivery rates. Journal of the American Chemical Society. 2012 Feb 1;134(4):2016-9.

[18] Falde EJ, Freedman JD, Herrera VL, Yohe ST, Colson YL, Grinstaff MW. Layered superhydrophobic meshes for controlled drug release. Journal of controlled release. 2015 Sep 28;214:23-9.

[19] DeRisi JL, Iyer VR, Brown PO. Exploring the metabolic and genetic control of gene expression on a genomic scale. Science. 1997 Oct 24;278(5338):680-6.

[20] Gallardo BS, Gupta VK, Eagerton FD, Jong LI, Craig VS, Shah RR, Abbott NL. Electrochemical principles for active control of liquids on submillimeter scales. Science. 1999 Jan 1;283(5398):57-60.

[21] Unger MA, Chou HP, Thorsen T, Scherer A, Quake SR. Monolithic microfabricated valves and pumps by multilayer soft lithography. Science. 2000 Apr 7;288(5463):113-6.

[22] Chang ST, Paunov VN, Petsev DN, Velev OD. Remotely powered self-propelling particles and micropumps based on miniature diodes. Nature materials. 2007 Mar;6(3):235-40.

[23] Simon MG, Lin R, Fisher JS, Lee AP. A Laplace pressure based microfluidic trap for passive droplet trapping and controlled release. Biomicrofluidics. 2012 Mar 24;6(1):014110.

[24] Bechtel SE. The oscillation of slender elliptical inviscid and Newtonian jets: Effects of surface tension, inertia, viscosity, and gravity.

[25] Wang YN, Fu LM. Micropumps and biomedical applications–A review. Microelectronic Engineering. 2018 Aug 5;195:121-38.

[26] Javadi A, Habibi M, Taheri FS, Moulinet S, Bonn D. Effect of wetting on capillary pumping in microchannels. Scientific reports. 2013 Mar 11;3(1):1-6.

[27] Bruus H. Theoretical microfluidics. Oxford: Oxford university press; 2008 Jan.

[28] Ju J, Park JY, Kim KC, Kim H, Berthier E, Beebe DJ, Lee SH. Backward flow in a surface tension driven micropump. Journal of Micromechanics and Microengineering. 2008 Jul 4;18(8):087002.

[29] Xing S, Harake RS, Pan T. Droplet-driven transports on superhydrophobic-patterned surface microfluidics. Lab on a Chip. 2011;11(21):3642-8.

[30] Javadi K, Moezzi-Rafie H, Goodarzi-Ardakani V, Javadi A, Miller R. Flow physics exploration of surface tension driven flows. Colloids and Surfaces A: Physicochemical and Engineering Aspects. 2017 Apr 5;518:30-45.

[31] Karbalaei A, Kumar R, Cho HJ. Thermocapillarity in microfluidics—A review. Micromachines. 2016 Jan;7(1):13.